AIAA JOURNAL
Vol. 30, No. 2, February 1992

Sound Transmission Through a High-Temperature Acoustic Probe Tube

Tony L. Parrott* and William E. Zorumski†
NASA Langley Research Center, Hampton, Virginia 23665

An investigation was conducted of acoustic transmission through a tube subjected to intense thermal gradients (50 K · mm^{-1}) along its axis. The results are of interest in the interpretation of acoustic data from probe tube configurations designed to measure fluctuating pressures in high-temperature environments. The measured transfer function across a localized heated region in the tube was compared to a computed transfer function based on a theoretical analysis of propagation through strong temperature gradients. The heated region of the tube was produced by a specially designed concentric heater located at the midspan of the tube between two measurement microphones. Over the frequency range 0.4–6.0 kHz, generally good agreement was obtained between the measured and calculated attenuation across the heated region with some discrepancy occurring at the attenuation minima. Agreement between measured and calculated phase difference was excellent to within the measurement resolution.

Introduction

ACCURATE fluctuating pressure data are needed to define dynamic loads on critical areas of hypersonic vehicles. These loads, which may involve turbulent boundary layers, shock/boundary-layer interaction, and combustion noise, cannot be predicted with sufficient accuracy for efficient structural designs. Therefore the design of such structures must rely on directly measured fluctuating loads data.[1] At hypersonic speeds, gas temperatures may exceed 2000 K in the sublayer. Such temperatures preclude direct flush mounts for currently available transducers, which are limited to about 600 K, unless active cooling is designed into the installation.[2] Aside from its invasive nature, active cooling is mechanically inconvenient and may subject the transducers to large thermal gradients that can alter the response in unknown or difficult to determine ways.

An alternate way to insure transducer survival and to maintain response stability is to remove the transducer from the immediate vicinity of the hostile environment via small-diameter transmission lines. These techniques, while far from satisfactory, must be used until high-temperature transducers are developed. If the aerothermal environment of such transmission line/transducer systems can be defined, then accurate, high-frequency measurements in hostile environments may be possible. Several investigators have examined the transmission characteristics of both "finite" and "infinite line" transducer systems with encouraging success.[3,4] For high-temperature environments, Ref. 3 suggests a water cooling jacket located between the transducer and probe end. Such an arrangement is more convenient and less invasive than actively cooled-flush-mount arrangements. However, the effects of strong thermal gradients in the transmission line have not been addressed.

This paper presents the results of a study undertaken to assess the effects of high-temperature gradients on propagation in an acoustic probe tube. The intent is to develop a transfer-function model for correcting acoustic data obtained in a high-temperature environment where the probe sensing end is located in the hot environment and the transducer is located at the cool end. Between the hot and cool ends a thermal gradient will exist which may be severe. To validate a transfer-function model that includes strong thermal gradient effects, an elevated temperature region with accompanying gradients was induced along the axis of a quartz tube and the transfer function across the region was measured.

The essential physics underlying the predictive model is wave reflection caused by changing gradients in the propagation medium. In particular, sound waves propagating through a gas are reflected by changing temperature gradients. Wave reflection in a medium with continuous variation of sound speed has received attention for over a hundred years. Young[5] published the exact solution for optical waves propagating in a medium with linearly varying speed in 1880.

Rayleigh[6] utilized Young's result in the description of waves on a string with variable density. Epstein[7] found analytic solutions for waves propagating through layers with speed variations expressed by exponential functions. In the Epstein layers, the speed and all of its derivatives are continuous. Layered media models,[8] with constant speed within each layer, are used to approximate the effects of continuous variations of sound speed.

In this paper, an analysis based on piecewise linear variation of the sound speed is exploited. The genesis of this method is found in a paper by Gingold[9] who developed uniformly valid solutions for a broad class of second-order differential equations, including those with turning points. The piecewise linear modeling is based on the availability of discrete, rather than continuous, temperature data within the probe tube. Gingold et al.[10] have shown that the general equation solution method reduces to an effective numerical method based on discrete temperature data.

The following section describes the apparatus and procedure used in the transmission experiments. This is followed by a description of the numerical method used to compute transmission and reflection coefficients for the hot section, and a comparison of computations with experiments. The experiments and data represent a portion of a M.S. thesis by Parrott.[11]

Description of Experiment

Test Apparatus

The experimental apparatus and instrumentation is shown in Fig. 1. The apparatus consisted of a 1.2 m length of fused

Received Sept. 6, 1990; presented as Paper 90-3991 at the AIAA 13th Aeroacoustics Conference, Tallahassee, FL, Oct. 22–24, 1990; revision received March 6, 1991; accepted for publication April 16, 1991.

*Research Scientist, Applied Acoustics Branch, Acoustics Division, Mail Stop 460.
†Chief Scientist, Acoustics Division, Mail Stop 462.

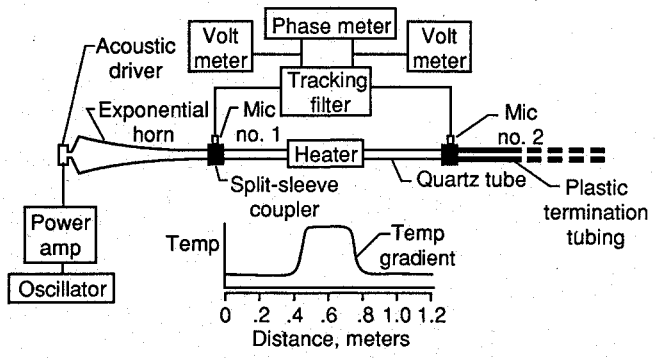

Fig. 1 Experimental setup and instrumentation.

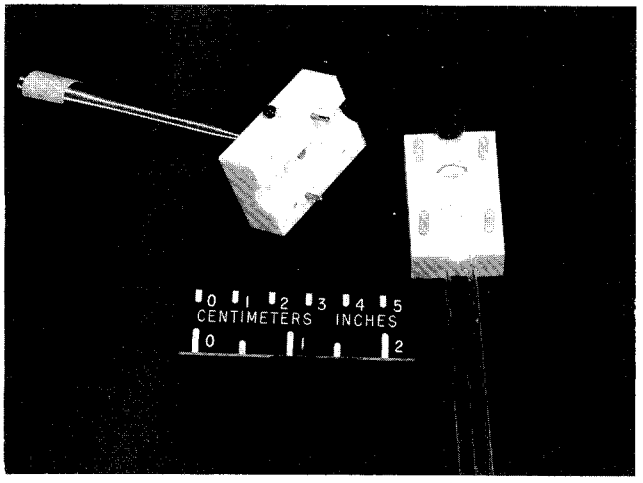

Fig. 2 Split-sleeve coupler.

quartz tube with a 0.15 m long concentric electric heater located near the midspan. The tube, with 7-mm inside diameter, was coupled to an electromagnetic driver capable of generating sound pressure levels in excess of 100 dB in the tube over the frequency range 0.2–6 kHz. The tube was coupled to the acoustic driver and a nonreflecting termination by specially designed, split-sleeve couplers. The nonreflecting termination consisted of a long length of plastic tubing with inside diameter chosen to match, as nearly as possible, that of the quartz tube.

Note that this experimental configuration was chosen for convenience to validate the mathematical model discussed later in this paper. In an actual probe tube configuration, sound will propagate from the probe entrance, at an elevated temperature, to the relatively cooler end where the transducer is located. The analytical model proposed in this paper may be used to correct such probe measurements for the effects of strong gradients along the probe axis as might exist when water cooling jackets are used to keep the probe short and to safegard the transducer from thermal inputs. It is assumed that a validation of the analytical model for the present experimental configuration would justify its application to the more realistic probe tube situation.

Microphone Installation

In addition to coupling the quartz tube to the source and termination, the split-sleeve couplers provided a means of installing the $^1/_8$ in. (3 mm) condenser microphones as shown in Fig. 2. Because area discontinuities in the propagation path between the measurement microphones will cause unwanted reflections, every attempt was made to minimize area disruptions associated with the microphone installation. Some area disruption is unavoidable however, which is illustrated in the scaled diagram of Fig. 3. The figure displays the range of possible microphone diaphragm locations relative to the inside diameter of the split sleeve. The maximum blockage (shaded area) and area expansion (bounded by dashed line) due to out-of-flushness are approximately 2 and 1%, respectively, of the total cross-sectional area. Also, a small discontinuity occurred at the junctures of the quartz tube with the shoulders of the split sleeve (see Fig. 2).

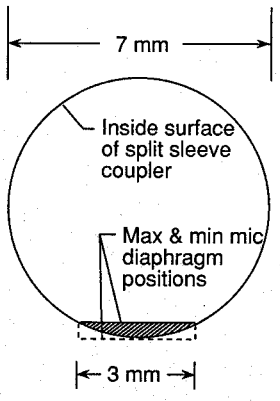

Fig. 3 Area disruption due to microphone installation.

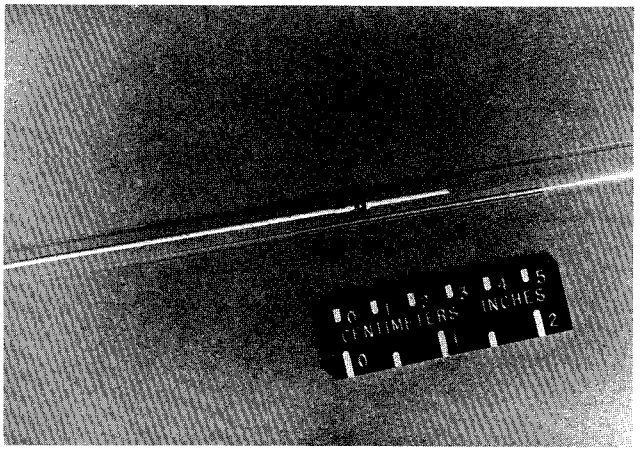

Fig. 4 Thermocouple probe in quartz tube.

Electric Heater Design

An electric heater was designed to produce a heated region along a 0.15 m length of the tube axis, as depicted in Fig. 1. The heating element consisted of a 3.5 m length of platinum wire embedded in an aluminum oxide casting formed on a mandrel sized to permit sliding contact of the heater with the quartz tube. The outside surface of the heater was wrapped in thermal insulation to reduce heat loss. With this arrangement, a maximum temperature of 1350 K could be achieved inside the tube. This temperature was about 96% of the annealing point temperature of quartz. Radial variation of temperature within the tube was estimated to be less than 3 K.

Heater current was controlled by a variac. Power input to the heater was monitored by measuring current and voltage. Two to three hours were allowed for the experimental setup to reach a thermal steady state before measurements were commenced. During the several hours required for a test sequence, line voltage variations of up to 10% could be reduced to about 2% by manual adjustment of the variac.

Temperature-Profile Measurement

Temperature profiles along the tube axis were measured with a thermocouple positioned incrementally along the tube axis in 5- or 10-mm steps with a positioning accuracy of approximately ±0.5 mm at the scale pointer. (This does not include error due to thermal expansion.) Figure 4 shows the thermocouple probe inserted into the quartz tube. The thermocouple

probe consisted of a chrome-alumel junction with lead wires embedded in a supporting probe sheath made of low thermally conducting material to reduce perturbing effects on the temperature profiles in high-gradient regions. Temperature was read manually to an accuracy of ±0.5 K. With this arrangement, a maximum temperature of 1350 K and a gradient of 50 K · mm^{-1} were measured. Variability of the temperature measurements between consecutive scans of the temperature profile was ±5 K in the high-gradient region. Reversing the probe direction yielded a perceptible shift in the profile shoulders but the shape was essentially unchanged. The ambient temperature varied from 295 to 298 K during the experiments.

Acoustic Measurements

Signals from the condenser microphones were appropriately conditioned and fed into a two-channel, 5-Hz bandwidth tracking filter. The filtered output voltages, proportional to the acoustic pressures, were measured with rms digital voltmeters to within ±1 mV accuracy. The phase difference between the signals was read by an analog phase meter to within ±1 deg. In addition to absolute calibration of the incident side microphone, relative amplitude and phase-response measurements between the two microphone channels were conducted. This was accomplished by installing the two microphones diametrically opposite each other in a single split sleeve. Overall variability in the relative response obtained in this way was about 0.3 dB in amplitude and 5 deg in phase between pretest and post-test calibrations. A large part of the variability was likely due to small variations in microphone mounting conditions and quartz tube coupling with the split sleeve.

Test Procedure

A typical transfer-function measurement consisted of about 85 frequencies taken at steps of 100 Hz (50 Hz for rapid changes) over the frequency range 0.4–6 kHz. Although the actual transfer-function measurements could be accomplished in less than 1 hour, test preparation would typically take several hours. The preparation steps consisted of relative response calibration of the microphone systems, attainment of thermal equilibrium for the elevated temperature region of the tube, measurement of the temperature profile, and installation of the split-sleeve couplers and microphones.

Probe Tube Transmission Analysis

The gas in the probe is at constant pressure p_0 but has spatially varying temperature $T(x)$, where x is the distance along the tube axis. The temperature is continuous but is known only at the measurement points so that some model must be adopted for the temperature variation between points. We assume linear variation of the sound speed between the data points. The speed of sound is a function of temperature so that it must be continuous also, with a possible discontinuous first derivative. The ambient temperature is designated by T_0 and the corresponding sound speed is c_0.

The time dependence of acoustic waves in this gas is given by the complex harmonic convention $\exp(-i\omega t)$, where ω is the circular frequency and t is time. In applications, there will be a natural length unit L and the acoustic equations are expressed in terms of this unit and the average state variables for the gas. Thus, $(x/L) \leftarrow x$, and $(\omega L/c_0) \leftarrow \omega$, where the symbol "$\leftarrow$" means that the variable on the right replaces the nondimensional group on the left. Since $\rho c^2 = \gamma p_0$ is constant, where $\rho(x)$ and $c(x)$ are the density and sound speed, respectively, and γ is the ratio of specific heats of the gas, the continuity and energy equations may be combined. This combined equation and the momentum equation give the following two-by-two first-order system:

$$\frac{d}{dx}\begin{Bmatrix}\hat{u}\\ \hat{p}\end{Bmatrix} = i\omega\begin{bmatrix}0 & 1\\ c^{-2} & 0\end{bmatrix}\begin{Bmatrix}\hat{u}\\ \hat{p}\end{Bmatrix} \tag{1}$$

where $\hat{u}$ and $\hat{p}$ are the nondimensional velocity and pressure fluctuations in the probe. This first-order system is valid for the strong temperature gradients expected in this investigation.

The transformation given in Ref. 8 takes the differential system, Eq. (1), into one with a symmetric coefficient matrix. This transformation amounts to a decomposition into progressive and regressive waves $\exp(\pm i\omega x/c)$ with the Wentzel-Kramers-Brillouin (WKB) amplitude factors $c^{\pm 1/2}$ for velocity and pressure.

$$\begin{Bmatrix}\hat{u}\\ \hat{p}\end{Bmatrix} = \begin{bmatrix}c^{1/2} & -c^{1/2}\\ c^{-1/2} & c^{-1/2}\end{bmatrix}\begin{Bmatrix}\hat{f}_0\\ \hat{g}_0\end{Bmatrix} \tag{2}$$

When the sound speed is constant, the new dependent variables can be interpreted as progressive and regressive wave amplitudes. The signs within the transformation matrix are chosen such that pressure is given by adding the waves and velocity is given by subtracting. When the sound speed is not constant, the new variables are defined by the differential system

$$\frac{d}{dx}\begin{Bmatrix}\hat{f}_0\\ \hat{g}_0\end{Bmatrix} = \begin{bmatrix}\dfrac{i\omega}{c} & \dfrac{1}{2}\dfrac{c'}{c}\\ \dfrac{1}{2}\dfrac{c'}{c} & -\dfrac{i\omega}{c}\end{bmatrix}\begin{Bmatrix}\hat{f}_0\\ \hat{g}_0\end{Bmatrix} \tag{3}$$

The off-diagonal elements in Eq. (3) are interpreted to be differential reflections caused by the sound-speed gradient.

A measure of the steepness of the sound-speed gradient, on the scale of a wavelength, is given by the following parameter:

$$\nu = c'/2\omega \tag{4}$$

This parameter is used in a second transformation of the dependent variable vector which incorporates the reflection effects of Eq. (3) into the vector:

$$\mu = \left(\frac{1+\nu}{1-\nu}\right)^{1/4} \tag{5}$$

$$\begin{Bmatrix}\hat{f}_0\\ \hat{g}_0\end{Bmatrix} = \frac{1}{2}\begin{bmatrix}(\mu+\mu^{-1}) & i(\mu-\mu^{-1})\\ -i(\mu-\mu^{-1}) & (\mu+\mu^{-1})\end{bmatrix}\begin{Bmatrix}\hat{f}_1\\ \hat{g}_1\end{Bmatrix} \tag{6}$$

The variable μ is nonzero and finite as long as the complex sound speed has an imaginary component. This imaginary component represents the attenuation of waves propagating through the tube. The new dependent variables are defined by the differential system:

$$\frac{d}{dx}\begin{Bmatrix}\hat{f}_1\\ \hat{g}_1\end{Bmatrix} = i\begin{bmatrix}\omega\tau' & -r\\ r & -\omega\tau'\end{bmatrix}\begin{Bmatrix}\hat{f}_1\\ \hat{g}_1\end{Bmatrix} \tag{7}$$

$$\tau = \int_0^x \frac{\sqrt{1-\nu^2}}{c}\,ds \tag{8}$$

$$r = \frac{1}{4\omega}\frac{c''}{1-\nu^2} \tag{9}$$

The differential reflection function r in Eq. (7) is proportional to the second derivative of the sound speed.

A final transformation is used to express the solution of Eq. (3) in terms of the "first-order gradient waves," $\exp(\pm i\omega\tau)$, and an amplitude matrix.

$$\begin{Bmatrix}\hat{f}_1\\ \hat{g}_1\end{Bmatrix} = \begin{bmatrix}e^{i\omega\tau} & 0\\ 0 & e^{-i\omega\tau}\end{bmatrix}\begin{bmatrix}a_{11} & -ia_{12}\\ ia_{21} & a_{22}\end{bmatrix}\begin{Bmatrix}C_1\\ C_2\end{Bmatrix} \tag{10}$$

The constants C_1 and C_2 may be selected to satisfy appropriate

boundary conditions. The imaginary factors $\pm i$ in the above transformation are inserted for convenience.

Direct substitution shows that the amplitude matrix satisfies the following differential system:

$$\frac{d}{dx}\begin{bmatrix} a_{11} & a_{12} \\ a_{21} & a_{22} \end{bmatrix} = r\begin{bmatrix} 0 & e^{-2i\omega\tau} \\ e^{2i\omega\tau} & 0 \end{bmatrix}\begin{bmatrix} a_{11} & a_{12} \\ a_{21} & a_{22} \end{bmatrix} \tag{11}$$

Initial conditions $a_{jk}(0) = \delta_{jk}$ are selected for Eq. (11) so that the constants in Eq. (10) represent the amplitudes of the first-order gradient waves at the origin. The amplitude matrix is constant between data points where the sound speed is assumed to vary linearly.

Reference 10 gives a numerical method for integrating Eq. (11). The method assumes that the sound speed varies linearly between the discrete data points of the measured temperature profiles. A parameter θ gives a compact expression for the local reflection function r.

$$\theta = \arcsin\nu \tag{12}$$

The local reflection function r is half of the derivative of θ.

$$r = {}^1/_2\theta' \tag{13}$$

The transmission time function τ is continuous and can be treated as a constant while integrating Eq. (11) in the neighborhoods of the discrete data points of the measured temperature profile. This integration gives a matrix recurrence formula relating the amplitude matrix in adjacent intervals

$$\begin{bmatrix} a_{11} & a_{12} \\ a_{21} & a_{22} \end{bmatrix}_{x_n+} = \begin{bmatrix} \cosh\frac{\Delta\theta_n}{2} & e^{-i\omega\tau_n}\sinh\frac{\Delta\theta_n}{2} \\ e^{i\omega\tau_n}\sinh\frac{\Delta\theta_n}{2} & \cosh\frac{\Delta\theta_n}{2} \end{bmatrix} \times \begin{bmatrix} a_{11} & a_{12} \\ a_{21} & a_{22} \end{bmatrix}_{x_n-} \tag{14}$$

$$\Delta\theta_n = \theta(x_n+) - \theta(x_n-) \tag{15}$$

The amplitude matrix is equal to the identity matrix in the interval containing the origin, so that the above formula is applied to step outward from that interval. The inverse transformation matrix required for stepping to lesser values of x is given by changing the sign of the off-diagonal terms.

The total pressure at microphone 2 was measured relative to microphone 1 in the experiment. Either constant in Eq. (10) may be assigned a unit value for purposes of similar relative pressure calculations. We let $C_1 = 1$ and computed C_2 from the termination impedance at microphone 2. The nondimensional termination impedance was nearly, but not exactly, unity. The quartz tube was slightly smaller than the plastic tube (area ratio 0.923) so a termination impedance was computed for the area expansion. This impedance Z_2 gives the constant C_2 from the termination impedance equation for the tube.

$$[Z_2 \quad -1]\begin{Bmatrix} \hat{u} \\ \hat{p} \end{Bmatrix} = 0 \tag{16}$$

The constants so determined were used to compute the relative complex pressure. Computed relative pressure levels and phase differences were computed for the highest temperature profile achievable in the quartz tube. These comparisons are presented in the Results and Discussion section that follows.

Results and Discussion

Dissipation Effects

Small-diameter tubes exhibit attenuation and reduced sound speed associated with visco-thermal dissipation in the acoustic boundary layer at the tube wall. These effects are described adequately by the classical Helmholtz-Kirchhoff theory[12] and are implicit in the transmission model discussed in the foregoing section. Prior to inducing thermal gradients in the quartz tube, the Helmholtz-Kirchhoff theory was verified. This was accomplished by direct measurements of tube attenuation and sound speed at ambient temperature (i.e., no thermal gradients). The measurements were obtained with the same experimental setup as was used for the transfer-function measurements across the thermal gradient region as is shown in Fig. 1.

Figure 5 shows measured and calculated sound speeds for a constant ambient temperature. The circular symbols represent the sound speed calculated from phase measurements between the measurement microphones spaced approximately 1.2 m apart and for an ambient temperature of 298 K. The continuous curves represent sound speeds calculated for the ambient temperature as indicated. Experiment and theory are seen to agree within the limits of measurement error. Figure 6 shows similar results for the spatial attenuation rates expressed in decibels per meter. Here, calculated curves are shown for 294 K and 300 K which bracketed the ambient temperature of 298 K for the measurements. Again the agreement between experiment and theory is good with the exception of the two lowest frequencies that are low by approximately 0.3 dB/m. This discrepancy is probably due to measurement scatter since the tube length was very nearly 1 m and thus produced an attenuation of only about 1 dB at the lowest frequencies. These comparisons provided confidence that the Helmholtz-Kirchoff theory adequately described visco-thermal dissipation at the tube wall and should apply to strong gradient regions with appropriate adjustments of gas properties. Both real sound speed and attenuation rate

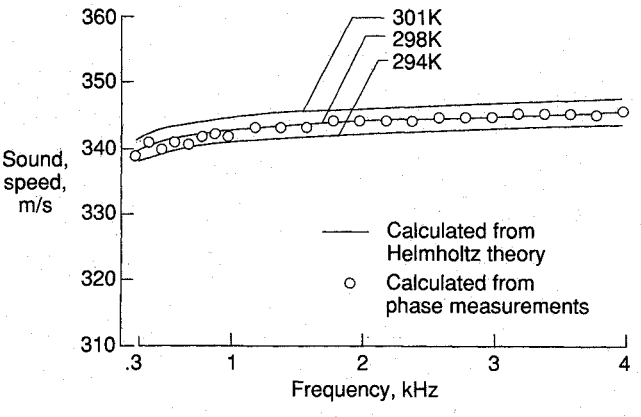

Fig. 5 Measured and calculated sound speed in tube.

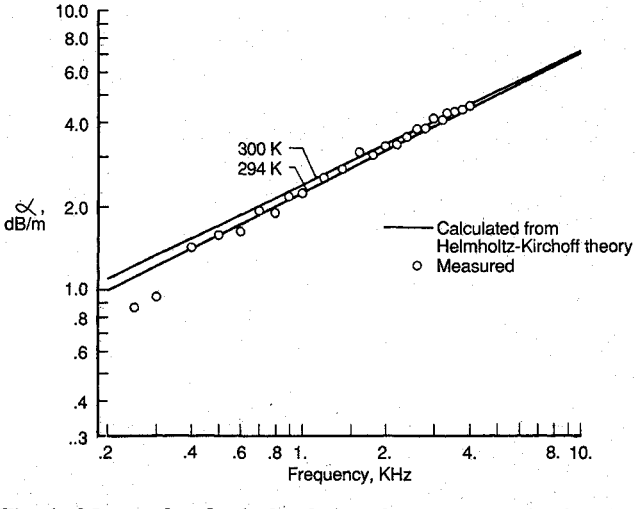

Fig. 6 Measured and calculated visco-thermal absorption in tube.

can be represented by defining the speed to be a complex variable.

Temperature Profiles

Figure 7 shows measured temperature profiles along the tube axis for three different temperature maxima. The profiles were constructed from discrete data taken every 10 mm (5 mm in high gradient regions). The profile plots are referenced to a temperature in the tube sufficiently distant from the heated region to be near the ambient temperature. The maximum temperatures are seen to range from 2.5 to 4.5 times the reference temperature. A feature of interest is the relatively small amount of spreading of the gradient region as the temperature is increased. Thus, all of the profiles are confined approximately to a length of 0.25 m or about 1.7 times heater length.

Idealized Temperature Profile

Before proceeding with a direct comparison of measured and calculated transfer functions for the actual temperature profiles shown in Fig. 7, it is instructive to consider the transmission characteristics of an idealized temperature profile as illustrated in Fig. 8. The feature of interest in this profile is the uniform, high-temperature region (hot spot) bounded by parabolic temperature distributions on either side (i.e., a linear sound-speed gradient). According to the theory developed above, sound reflections occur only where $c'' \neq 0$ or at the interfaces between regions I, II, III, IV, and V. In the absence of visco-thermal dissipation, the resulting wave equations can be solved in closed form. If the gradient region length is allowed to approach zero, this closed-form solution reduces to the well-known case for transmission through a three-layer medium.[12] The transmission loss maxima are then periodic in frequency as shown by the dashed curve of Fig. 9. In the same figure, the solid curve shows the transmission loss for the parabolic gradient bounded "hot spot." Here, the key feature of interest is the decrease in transmission loss maxima with increasinig frequency. Also, the maxima are shifted downward in frequency relative to the maxima for the discontinuity bounded hot spot.

If the transfer function is calculated for the parabolic gradient bounded hot spot, without visco-thermal dissipation, the attenuation component appears as shown in Fig. 10. The envelope of this curve corresponds to the transmission loss curve (solid) in Fig. 9. In effect, the attenuation can be imagined as a modulated version of the transmission loss curve generated by standing wave nulls passing over microphone 1 as the frequency is increased. The periodicity of the modulation corresponds to resonant frequencies associated with the separation distance between microphone 1 and the hot spot. For this calculation, the separation distance was about 0.34 m, which gives a periodicity of about 0.25 kHz. This compares favorably with that observed in Fig. 10.

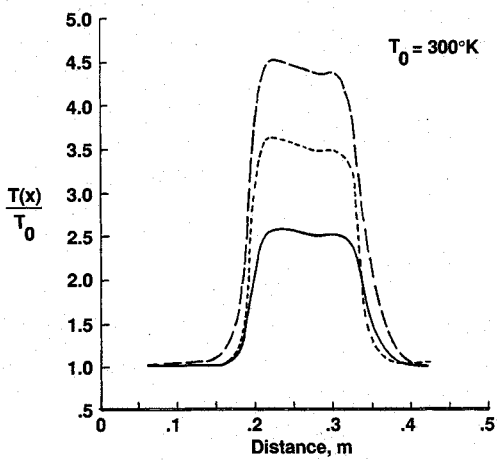

Fig. 7 Measured temperature profiles in quartz tube.

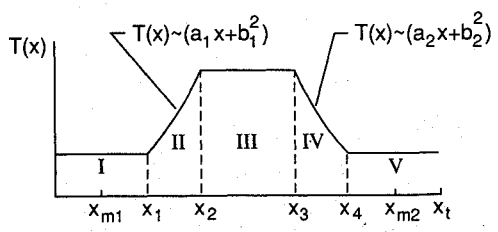

Fig. 8 Idealized temperature profile.

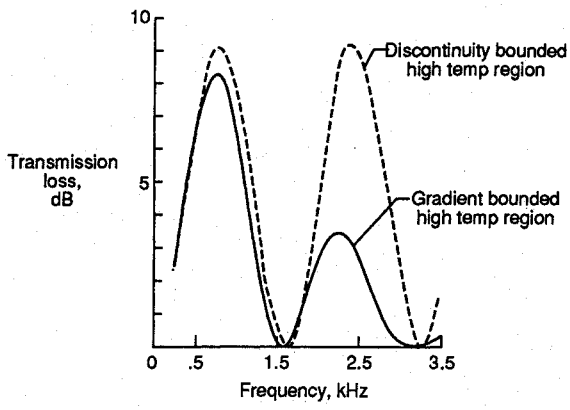

Fig. 9 Transmission losses for idealized profiles.

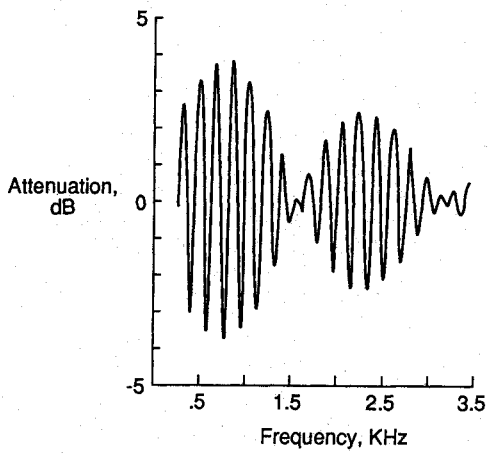

Fig. 10 Attenuation across idealized profile.

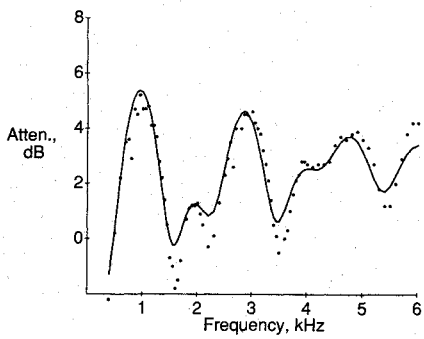

Fig. 11 Measured and calculated attenuation across temperature profile.

Transfer Functions

Figures 11 and 12 compare the measured and calculated transfer function for the intermediate temperature profile of Fig. 7. Figure 11 shows the attenuation component, and Fig. 12 shows the phase component. The microphone separation for this measurement was 0.344 m and the "hot" region was

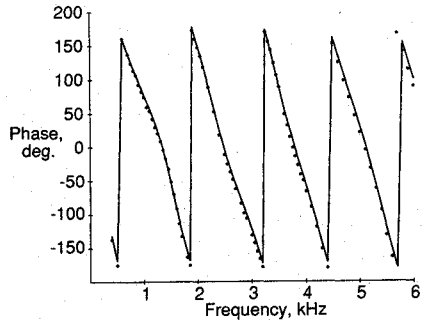

Fig. 12 Measured and calculated phase change across temperature profile.

approximately 0.1 m from microphone 1. The darkened symbols in the figures represent measurements and the continuous curves represent calculated results for a nonreflecting termination. Calculations were also performed for termination area discontinuities of up to 10% with no significant change in the results.

The general trends of the measured and calculated attenuation in Fig. 11 show good agreement. The major attenuation peaks occur near 1 kHz, 2.8 kHz, and 4.7 kHz. The second and third peaks at 2.8 kHz and 4.7 kHz are shifted downward from 3 kHz and 5 kHz, respectively, where they would occur for a discontinuity bounded hot region as discussed in Fig. 9. The modulations in the attenuation, so evident in the calculated result presented in Fig. 10, are not obvious here but are probably associated with the secondary peaks near 2 kHz and 4 kHz. The modulation periodicity in this case is approximately 0.86 kHz. Apparently, the more realistic features involving visco-thermal dissipation and asymmetry in the temperature profile have obscured the symmetrical attenuation pattern shown in Fig. 9.

Another observation of interest in Fig. 11 is that lower attenuation minima were consistently measured than were predicted. This feature may result from the fact that attenuation minima would always be negative, corresponding to a standing wave null over microphone 1, if it were not for the counter-effect of attenuation due to visco-thermal dissipation. Thus, at near zero net attenuation, these two effects are critically balanced, and the relative measurement error is at its worst. In view of these considerations, the agreement between measured and calculated attenuation is surprisingly good at the attenuation minima.

The agreement between calculated and measured phase in Fig. 12 appears to be excellent. It should be noted that the phase-measurement variability was about ±2.25 deg. Thus, the data symbol diameter approximately represents the measurement-variability range. It should also be noted that the perturbing effect of the hot region is mainly manifested at the lower frequencies (i.e., for a uniform temperature tube, and with no reflections, the phase would be linear with frequency). This observation is consistent with Eq. (4).

The results of this investigation suggest that the effect of strong temperature gradients on the acoustic transfer function of a probe tube can be accurately predicted. However, the predictive model must have accurate temperature-profile information and must include visco-thermal effects in the probe tube.

Concluding Remarks

This study shows that a theoretically derived transfer function may be used to correct data measured by a high-temperature acoustic probe tube. The analytical model is a one-dimensional strong-gradient acoustic equation with complex sound speed based on the classic Helmholtz-Kirchhoff theory. The model was validated by an experimental measurement of the transfer function across an elevated temperature region (1050 K) bounded by strong thermal gradients. Temperature gradients bounding the hot region were as large as 50 $K \cdot mm^{-1}$.

Agreement between the computed and measured attenuation was judged to be good and phase agreement was judged to be excellent over the frequency range from 0.4 to 6 kHz. The differences between the calculated and measured attenuation occurred mainly at attenuation minima and are attributed in large part to increased relative measurement error at these frequencies.

The results suggest that the predictive scheme can be successfully employed to correct microphone probe tube responses for the effects of large temperature gradients. Because probe tubes tend to be of small diameter, visco-thermal dissipation at the tube wall must be included for accurate response calculations.

References

[1]Holden, M. S., "A Review of Aerothermal Problems Associated with Hypersonic Flight," AIAA Paper 86-0267, Reno, NV, Jan. 1986.

[2]Heller, H. H., and Widnall, S. E., "Dynamics of an Acoustic Probe for Measuring Pressure Fluctuations on a Hypersonic Re-Entry Vehicle," *Journal of the Acoustical Society of America*, Vol. 44, No. 4, 1968, pp. 885–896.

[3]Englund, D. R., and Richards, W. B., "The Infinite Line Pressure Probe," *ISA Transactions*, Vol. 24, No. 2, Instrument Society of America, Research Triangle Park, NC, 1985, pp. 11–19.

[4]Salikuddin, R., Burrin, R., and Brown, W., "Design and Characterization of a High Temperature and High Frequency Infinite-Line Pressure Probe," AIAA Paper 89-1116, San Antonio, TX, April 1989.

[5]Rayleigh, J. W. S., *The Theory of Sound*, Vol. I, 2nd. Ed., Dover, New York, 1945, pp. 234, 235.

[6]Rayleigh, J. W. S., *The Theory of Sound*, Vol. I, 2nd ed., Dover, New York, 1945, pp. 235, 239.

[7]Burman, R., and Gould, R. N., "The Reflection of Waves in Generalized Epstein Profile," *Canadian Journal of Physics*, Vol. 43, May 1965, pp. 921–934.

[8]Brekhovskikh, L. M., *Waves in Layered Media*, 2nd ed. (translated by Robert T. Beyer), Academic, New York, 1980, Chap. II, Sec. 18.

[9]Gingold, H., "An Invariant Asymptotic Formula for Solutions of Second-Order Linear ode's," *Asymptotic Analysis*, Vol. 1, 1988, pp. 317–350.

[10]Gingold, H., She, J., and Zorumski, W. E., "Reflection of Sound Waves by Sound-Speed Inhomogeneities," *Journal of the Acoustical Society of America* (accepted for publication).

[11]Parrott, T. L., "Propagation of Sound Through Thermal Gradients Along the Axis of a Quartz Tube," M.S. Thesis, Mechanical Engineering, George Washington Univ., Washington, DC, Aug. 1973.

[12]Kinsler, K. E., and Frey, R. F., *Fundamentals of Acoustics*, 2nd ed., Wiley, New York, 1962, pp. 237–241.